

Nonlinear Dynamic Behavior of Two Distinct Chaotic Systems

Huda Hamdan Ali¹ and Hayder A. Naser^{2,*}

¹ Department of CTE, Imam Al-Kadhum College, Baghdad, Iraq. huda.hamdan33@gmail.com

² Department of CTE, Imam Al-Kadhum College, Baghdad, Iraq.

*Corresponding author: Hayder A. Naser², hayder.a.naser@gmail.com

Abstract

The nonlinear dynamics of two chaotic systems, namely the optoelectronic feedback (OEFB) and the Lu-Chen electronic chaotic system, are simulated and implemented in this work using the Berkeley Madonna software. Control parameters and initial conditions have been adjusted to demonstrate transitions from one state to another. Upon modifying certain regulating elements, both systems exhibited excessive sensitivity to initial conditions and displayed dynamic nonlinear behavior. The OEFB system reveals a homoclinic condition with a Shilnikov attractor as the feedback intensity increases. In contrast, the Lu-Chen system exhibits sensitivity to parameters a , b , and c , accompanied by multiscroll behavior, as evidenced by time series, the Fast Fourier Transform (FFT), and attractor analysis. These results offer potential applications, including data encoding, secure communications, and image processing. This research studied the properties of two different chaotic dynamical systems. These two chaotic systems are optoelectronic feedback and Chua systems. The results are analyzed, and it is found that the behavior of the Chua system changes in the time series, which in turn causes the attractor to change. The results showed a significant increase in the Chua system's bandwidth. Studying the different characteristics opens a broad scope for many applications, the most important of which is secure communications.

Keywords: Attractor; Chaotic method; Nonlinear system; OEFB; Chua systems; cryptographic

1. Introduction

Chaos theory has garnered significant attention since Lorenz first proposed it in 1963. Over the past decade, experiments have validated various approaches for generating optical chaos, including external optical feedback, optical injections, and external modulation (Luo et al., 2021). Chaotic systems exhibit hypersensitivity to initial conditions due to their non-periodic, noise-like wideband nature. This characteristic enables a deeper understanding of seemingly random systems (Jamal et al.2022). The design of hundreds of cryptographic primitives has utilized



chaos and nonlinear dynamics in recent decades (Li et al., 2009). Optoelectronic feedback (OEFB) systems exhibit nonlinearity in their dynamics, incorporating both optical and electrical components (Chengui et al., 2020). Optical physical systems are well-known for their intricate and unpredictable chaotic behavior, capable of introducing nonlinear delays (Jacquot et al., 2010). Prominent instances of three-dimensional independent chaotic flows encompass the Lorenz, Chen, Lü, and Laminar Chaos systems, characterized by the presence of one or more horseshoe or saddle focal points (Raied et al., 2016) (Müller-Bender et al., 2020). The Lu-Chen chaotic system, unveiled in 2002, emerged as a specific instance derived from the Lorenz system (Lü et al., 2002) and (Algaba et al., 2013), it holds a notable position in controlling nonlinear dynamical systems, with stability, optimality, and uncertainty being crucial areas of focus (Ibrahim et al., 2021). The manipulation of control parameters within the Lu-Chen system can impact the overall dynamics, representing a noteworthy outcome within control theory (Doungmo et al., 2021). Homoclinic orbits, an intriguing facet of chaotic systems as understood by Shil'nikov (Ueta et al., 2000), find applications in communications (Dina et al., 2016), the Internet of Things (IoT) devices, wireless communication (Li et al., 2006), and various engineering applications. (Wei et al., 2016) examine the multiple-delayed Wang-Chen system with concealed chaotic attractors through analytical and numerical methods. Wang (Wang et al., 2019) subsequently develop a novel inductor-free Chua's circuit for producing multi-scroll chaotic attractors. Pehlivan (Pehlivan et al., 2019) employed differential equations to adjust the scaling of a multiscroll chaotic Lu-Chen system. Trikh (Trikh et al., 2022) devised a synchronization technique utilizing fractional inverse matrix projective difference synchronization across three parallel chaotic fractional-order systems, grounded in Lyapunov stability theory. The fuzzy controller is used to control the behavior of the system based on the several control variables efficiently (Saini D, 2021). The synchronization of chaos in two QD-LEDs connected by a unidirectional and bidirectional coupling system is also examined in (Kadim et al., 2023). This study compared two chaotic systems with different behaviors, namely Lu-Chen and OEFB, using Chaos Tools and the Berkeley Madonna software.

2. Methods

In the OEFB system, a nonlinear optoelectronic configuration was considered. The photodetector receives the output laser light and generates a current proportionate to its optical intensity, as illustrated in Figure 1. The relevant signal passes through a variable gain amplifier before being looped back into the laser's injection current. The strength of the feedback is determined by the amplifier gain. The laser emits a continuous light of 5 mW at a wavelength of 632.8 nm. The dynamical sequence represented in the data is observed by maintaining a fixed DC-pump current and adjusting the feedback gain.

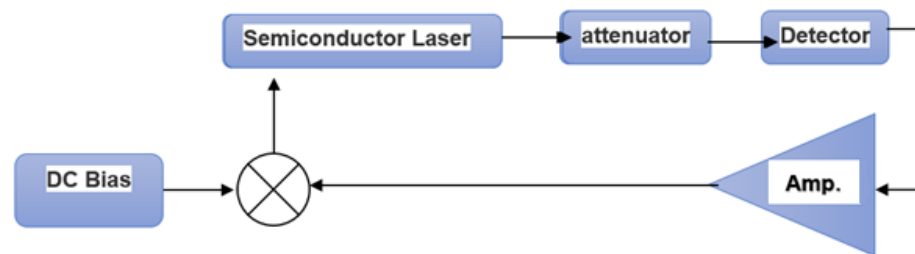


Figure 1: A sketch illustrating the proposed environment with the OEFB loop

The dynamics of photoelectric intensity and charge carriers can be described using the standard single-laser diode rate equations 1, 2, and 3, which have been modified to incorporate the current feedback system (Chow et al., 2012).

$$\frac{dx}{dt} = x(y - 1) \quad (1)$$

$$\frac{dy}{dt} = \gamma(\delta_0 - y + f(w + x) - xy) \quad (2)$$

$$\frac{dw}{dt} = \varepsilon(w + x) \quad (3)$$

Here, ε represents the feedback strength, δ_0 is the bias current, and γ is the proportion of the population relaxation rate. The intensity of the output laser ray is expressed in the first equation, while the second equation represents the inversion of the population. The third equation depicts the feedback necessary for chaos generation. The outcome is a tri slow-fast scheme that transitions from a steady stable form to regular intervals of spiking patterns as the current is altered. Due to the Lu-Chen system's dynamic limits surpassing those of the power supply, adjustments to the variables x , y , and z are essential for electronic circuit implementation and other real-time applications. The nonlinear equations of the Lu-Chen system are described in equations 4, 5, and 6 (Liu et al., 2003).

$$\frac{dx}{dt} = a \cdot x + d_1 \cdot y \cdot z \quad (4)$$

$$\frac{dy}{dt} = b \cdot y + d_2 \cdot x \cdot z \quad (5)$$

$$\frac{dz}{dt} = c \cdot z + d_3 \cdot x \cdot y \quad (6)$$

With two quadratic nonlinearity terms, these mathematical models describe a brand-new chaotic system in three dimensions. The typical parameter values for the chaotic system are d_1, d_2, d_3, a, b, c , which are -1, 1, 1, 5, -10, and -3, respectively. The initial conditions x_0, y_0, z_0 are set as -3, 0, 3, respectively. The Lu-Chen design is illustrated in Figure 2.

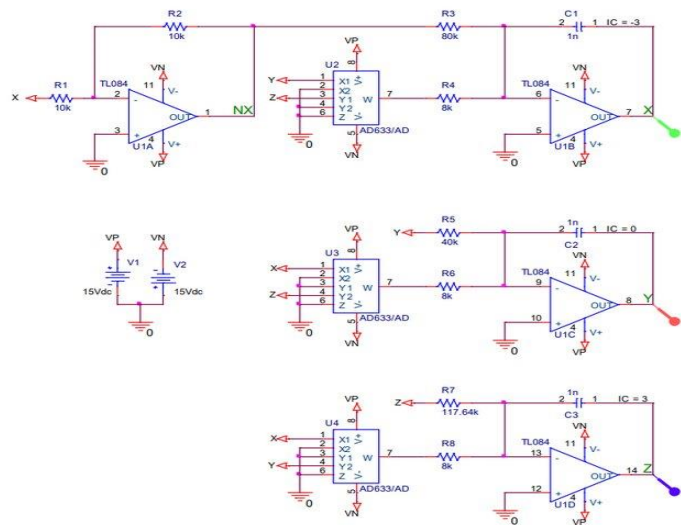


Figure 2: Schematic of the intended electronic oscillator of the Lu-Chen system (Pehlivan et al., 2019).

3. Results and discussions

3.1 Nonlinear behavior of OEFB system

The theoretical model of the nonlinear system is programmed by Berkeley Madonna software, Figure 3, with the bias current $\delta 0$ fixed at (1.01747), while ε is varied.

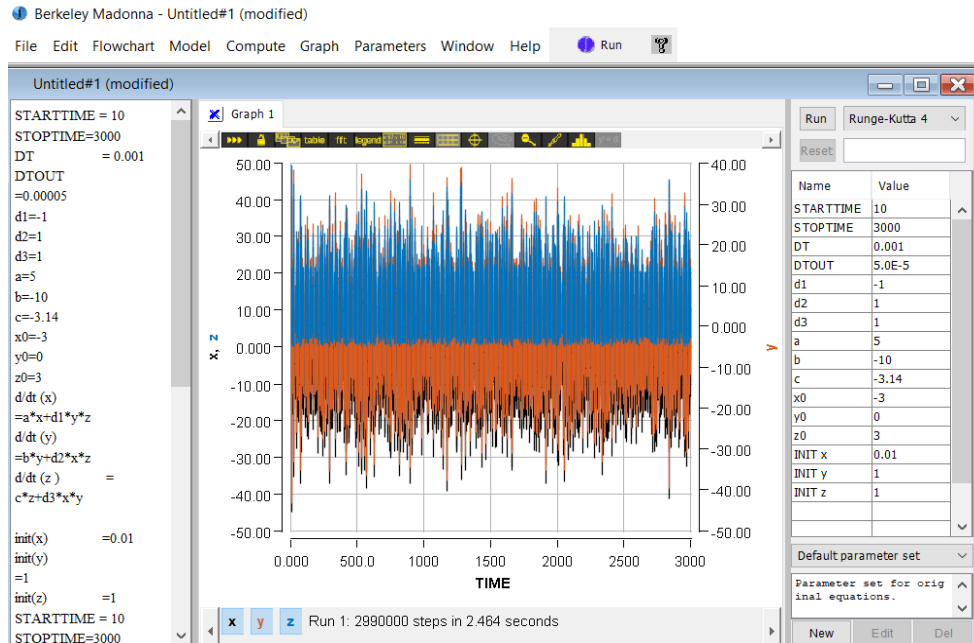
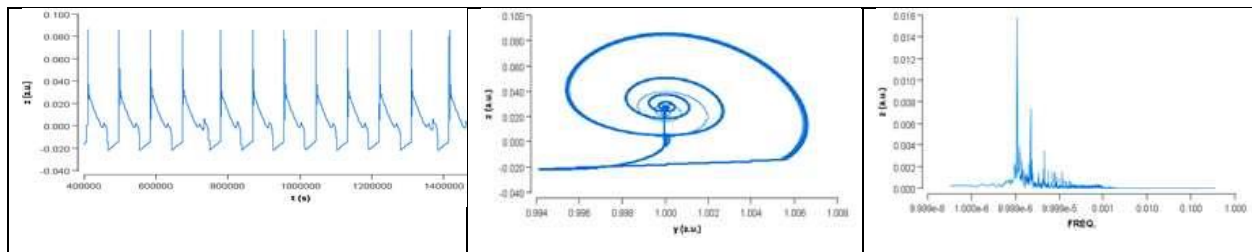


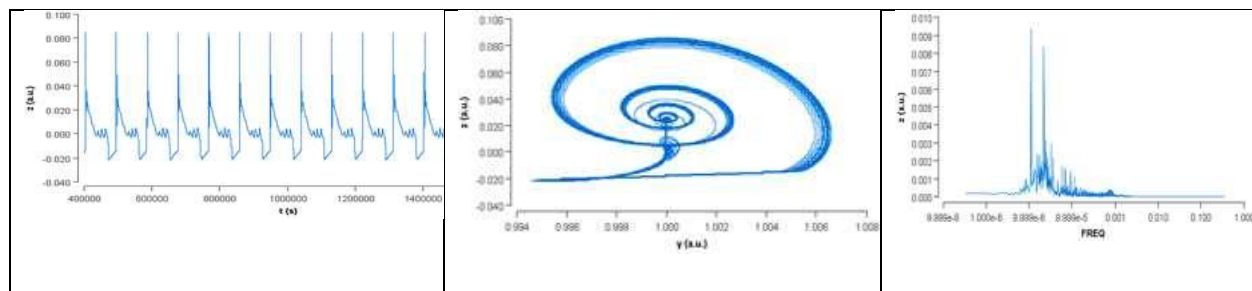
Figure 3: main window of Berkeley Madonna software

Other parameters are set as follows: $\gamma = 1 \times 10^{-3}$, $\alpha = 1$, $s = 11$, and the initial conditions are $x_1 = 0.022$, $y_1 = 1$, $z_1 = 0.005$. The system exhibits a series of steady, periodicity-doubling, and chaotic states with restricted intensity, as depicted in Figure 4. At the laser threshold, chaotic behavior arises from the interaction of the dense phase space, leading to a supercritical division. The static laser pulse waveform starts to lose stability just above the beam threshold due to a supercritical Hopf bifurcation.

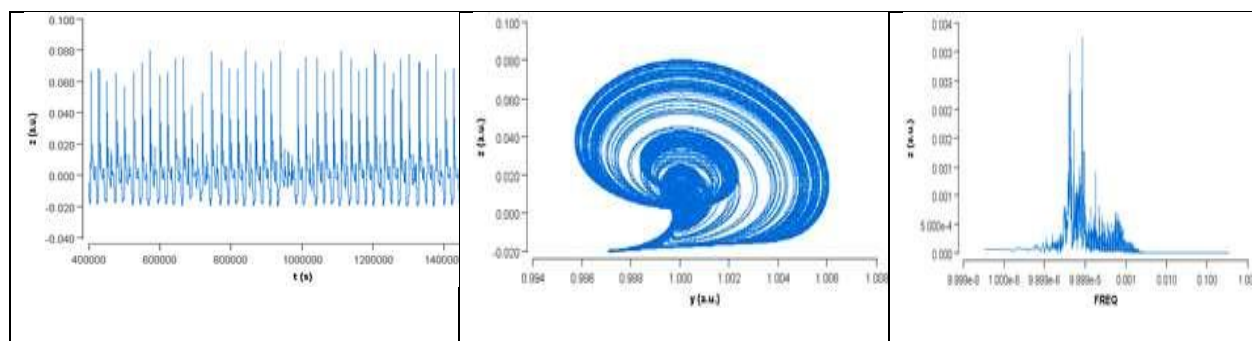
(a)



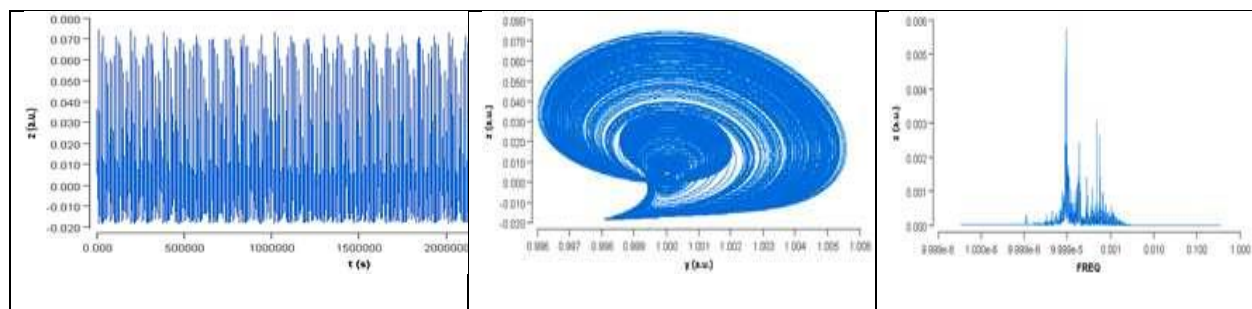
(b)



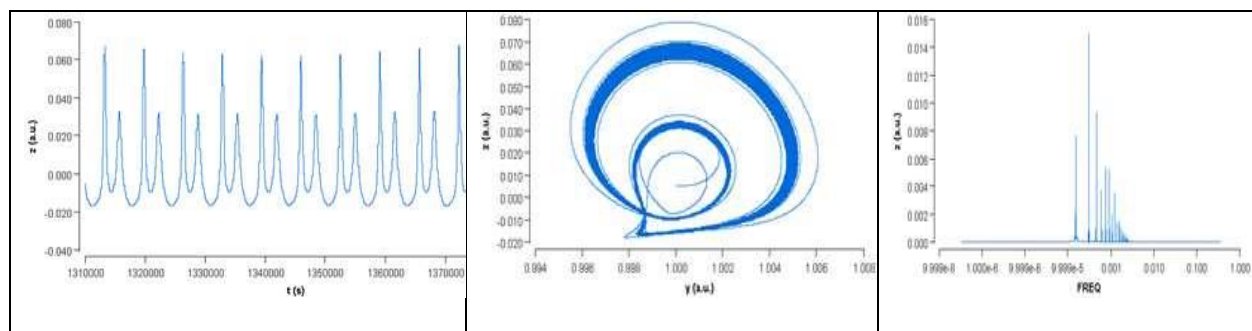
(c)



(d)



(e)



(f)

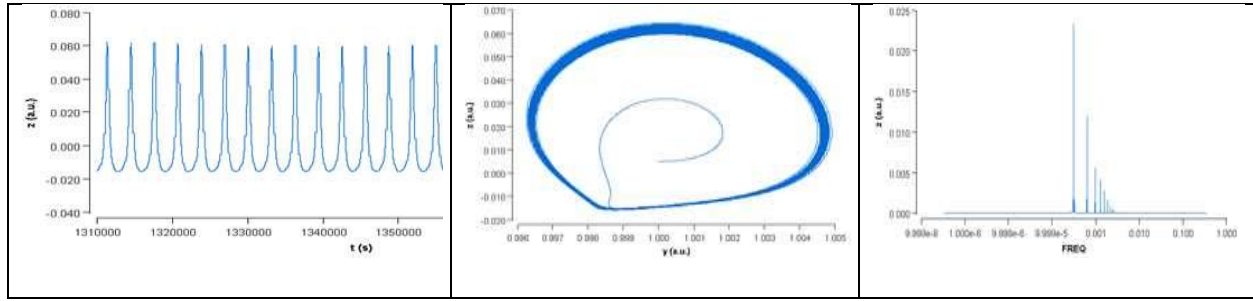


Figure 4: Z-Y phase of the OEFB system's response to feedback strength: (a) 1.5×10^{-5} , (b) 2.1×10^{-5} , (c) 7×10^{-5} , (d) 1.2×10^{-4} , (e) 2.3×10^{-4} , (f) 3×10^{-4} . The OEFB system exhibits excitable behavior during periodic, period doubling, and chaotic states.

Figure 4 depicts the nonlinear behavior of the OEFB system. Initially, it exhibits a limit cycle at (a). As the power increases (b), it transitions to a state of mixed-mode oscillations (MMOs), progressing through chaotic cases at (c) and (d), where the system demonstrates horseshoe-type or Shil'nikov chaos (Ren et al., 2010). The system then returns to period doubling and a periodic state at (e) and (f), respectively, while the feedback continues to increase. Furthermore, the system was observed to be excessively sensitive to initial conditions, as illustrated in Figure 5.

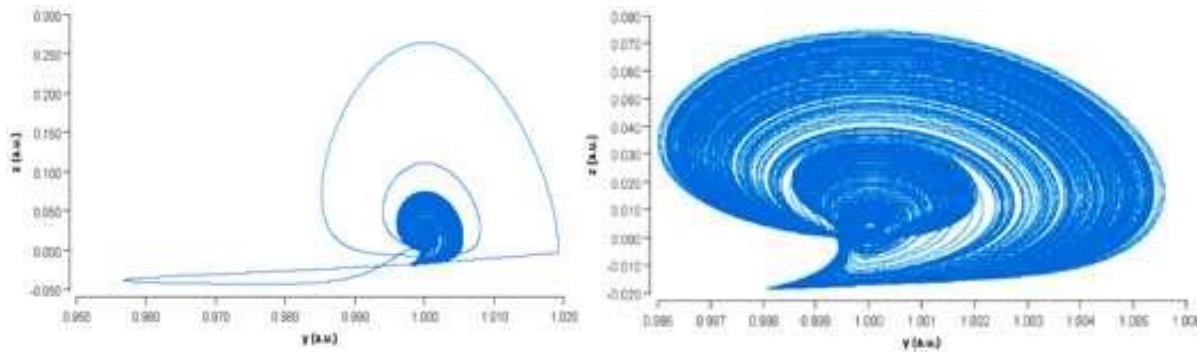


Figure 5. The sensitivity of the system to initial conditions with $x_1=0.05$ (right) and $x_1=0.022$ (left). The same numbers described above are used as other factors with $\varepsilon = 1.2 \times 10^{-4}$.

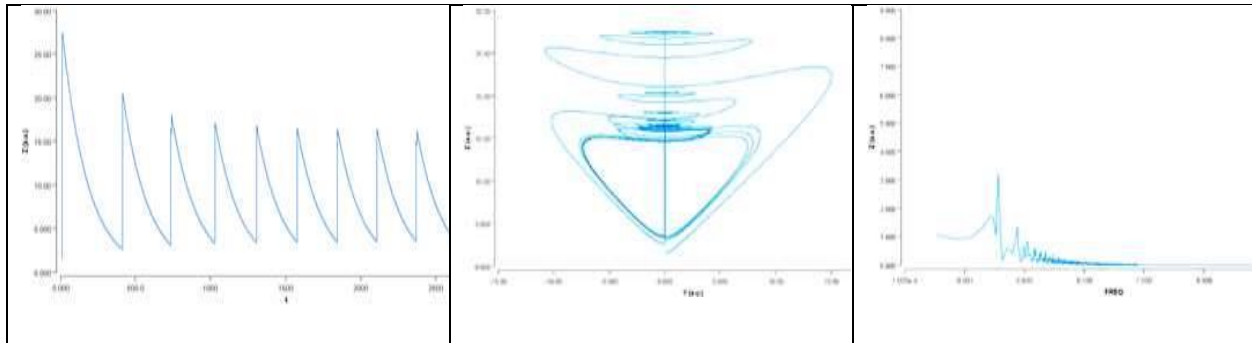
Based on the results of the previous paragraphs, we have determined that the period of the phase-space orbit is fully determined by the timescale split between the faster SL timescales and the slower AC feedback loop timescales. As feedback increases, this split decreases until it becomes too small to support slow-fast relaxation oscillations.

3.2 Nonlinear behavior of Lu-Chen system

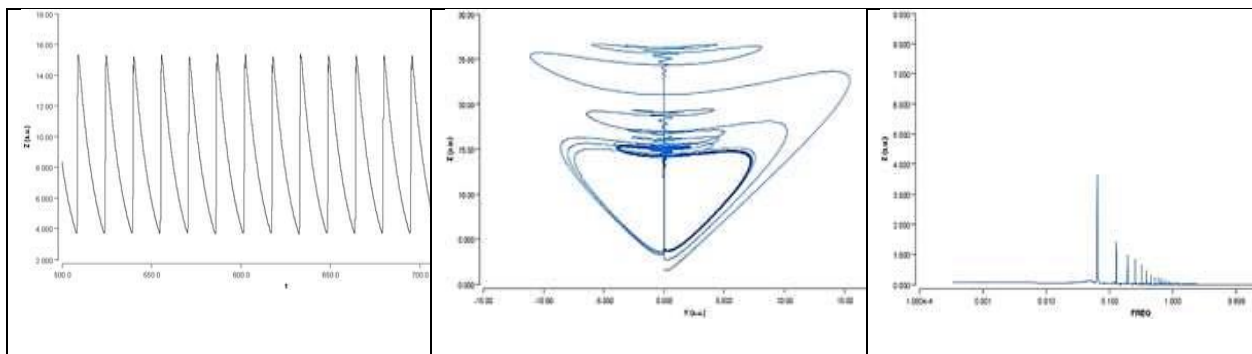
As a result of the simulation, Figure 6 depicts signals in x-y, z-y output phase, and an FFT. The initial conditions for this system, $\text{init}(x)$, $\text{init}(y)$, and $\text{init}(z)$, are set at 0.5, 1, and 1, respectively. The values of d_1 , d_2 , and d_3 are -9.55, 9.55, and 0.94, respectively. The capacity parameter (c) values were altered, while a and b are fixed at 4.54 and -9.5,

respectively. The initial values are $x_0 = -2.9$, $y_0 = 0.01$, and $z_0 = 2.8$. In comparison to the OEFB system, a multiscroll chaotic Lu-Chen system was scaled. According to the comparative simulation, the chaotic multiscroll-scaled Lu-Chen system exhibits successful scaling and can be implemented in an electronically manufactured circuit.

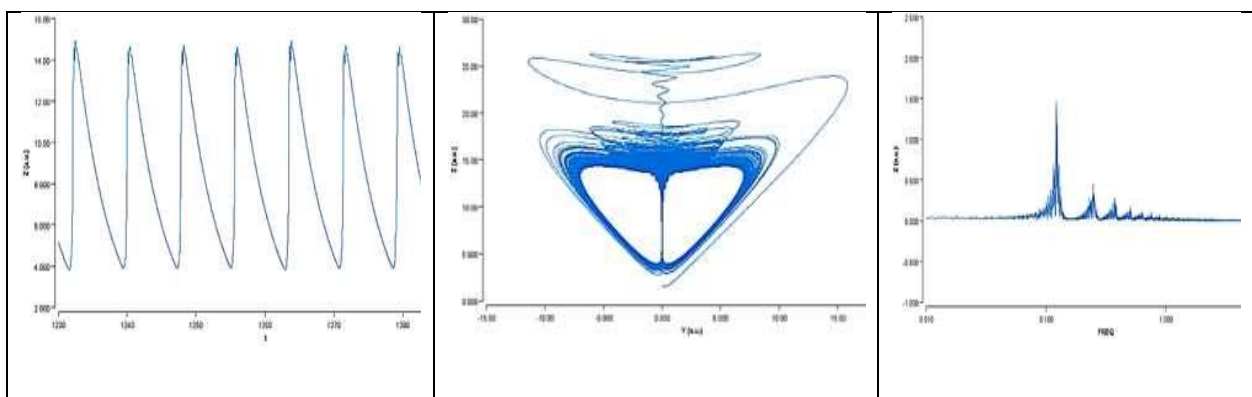
(a)



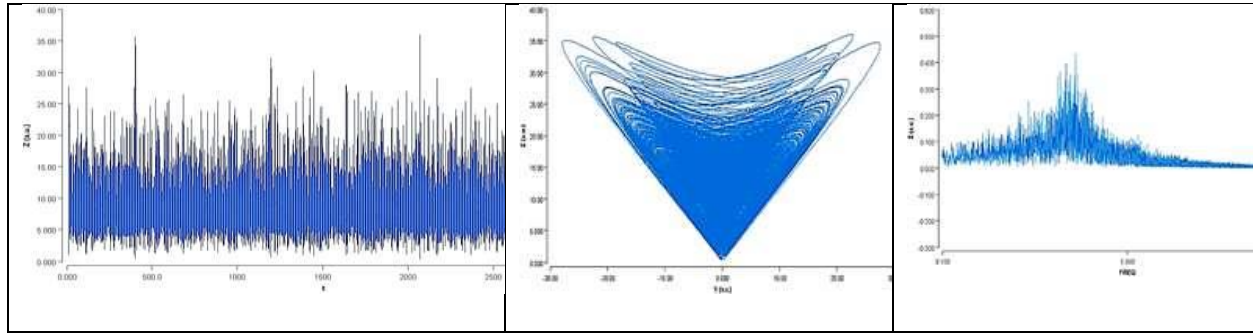
(b)



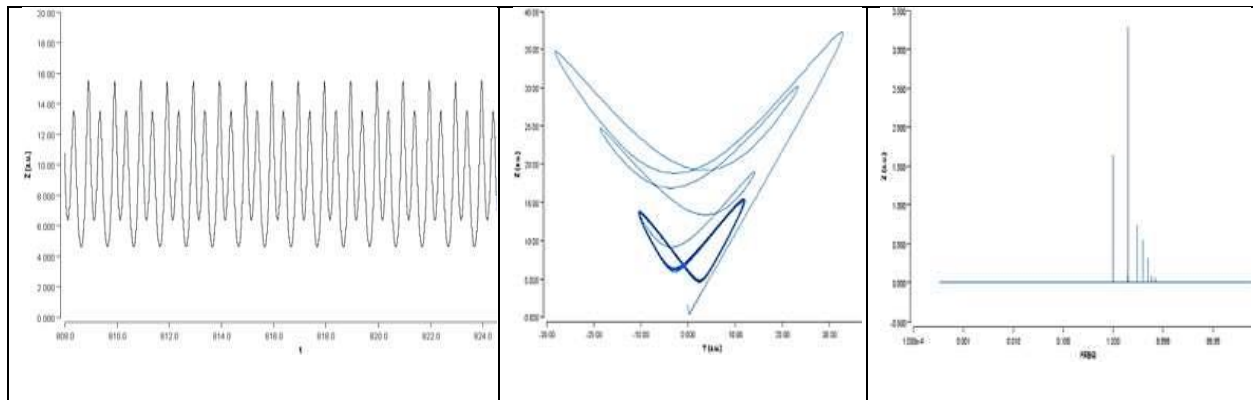
(c)



(d)



(e)



(f)

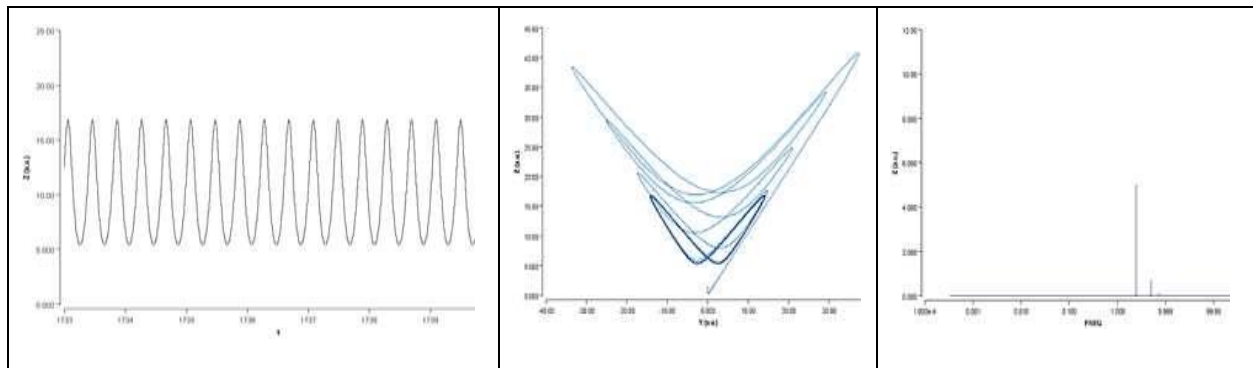


Figure 6: The Z-Y phase space at $\text{init}(x) = 0.5$, $\text{init}(y) = 1$, $\text{init}(z) = 1$, $d_1 = -9.55$, $d_2 = 9.55$, $d_3 = 0.94$, $a = 4.54$, $b = -9.5$, $x_0 = -2.9$, $y_0 = 0.01$, $z_0 = 2.8$ with c values: (a) -0.0059 , (b) -0.1 , (c) -0.2 limit cycle, (d) -1.5 , (e) -5.6 , (f) -5.8 respectively.

Figure 6 displays the nonlinear behavior of the Lu-Chen system, showcasing periodicity with decreasing c (a, b), transitioning to a limit cycle (c), followed by chaos (d), and returning to period doubling and periodic states (e, f). Additionally, as observed in Figure 7, the system has been found to be sensitive to initial conditions. These results are important to be used in the image encoded using computer generated hologram (CGH) technology (Hamadi et al., 2022).

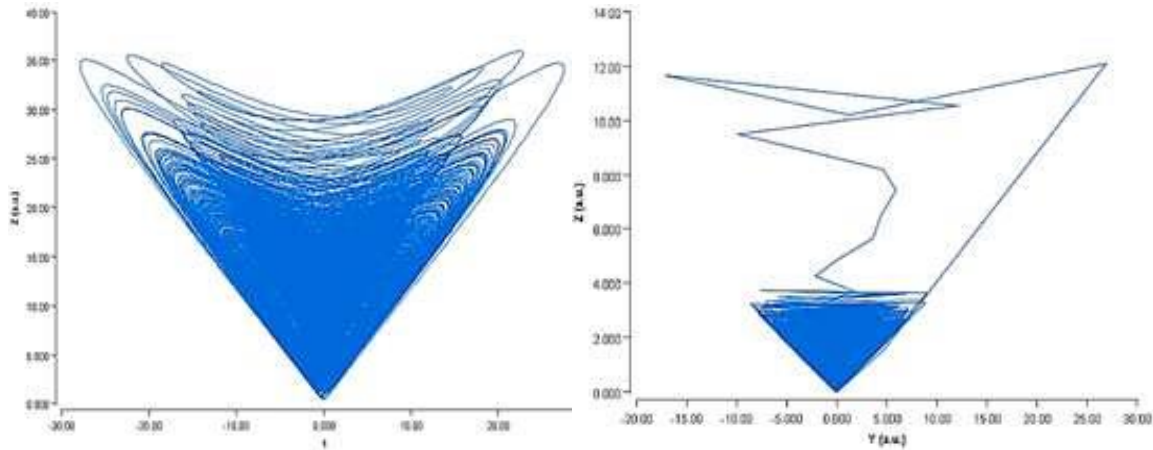


Figure 7: Sensitivity of the Lu-Chen system to shifting initial conditions $\text{init}(x)$, $\text{init}(y)$, and $\text{init}(z)$. Left: 0.5, 1, and 1, respectively. Right: 5×10^{-5} , 1×10^{-6} , and 1×10^{-5} , respectively. Other parameters with $c = -1.5$ utilize the same values as before.

There is a "double scroll" pattern for the Chua system attractor. Similar results are found when merging more than one chaotic system, as in (Jamal et al., 2021).

Table 1 illustrates the impact of feedback strength on the attractor shape.

Table 1: The effect of strength on the shape of the attractor for OEFB and Lu-Chen systems.

Shape of attractor	Feedback strength ε	Control parameter \odot
Steady state	Zero	zero
Limit cycle	1.5×10^{-5}	-0.2
Mmos	2.1×10^{-5}	-----
Chaotic	1.2×10^{-4}	-1.5
Period doubling	2.3×10^{-4}	-5.6
periodic	3×10^{-4}	-5.8

The behavior of the bifurcation diagrams for the two systems could be explored by detecting and isolating the peaks. These diagrams are shown in Figure 8.

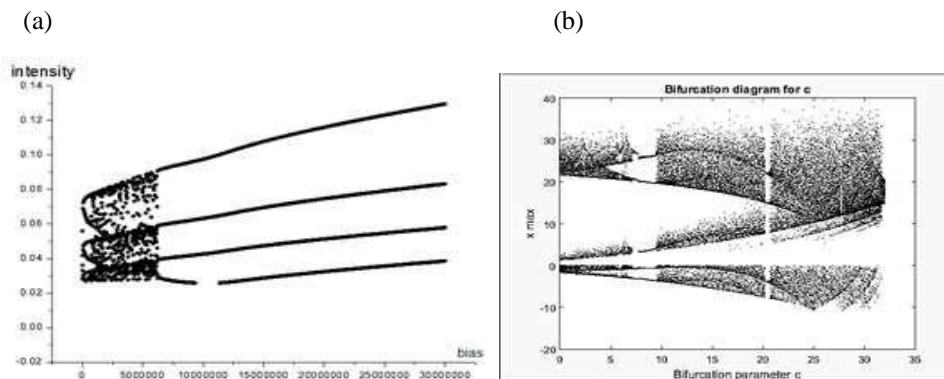


Figure 8: The bifurcation diagram for the OEFB model (left) and the Lu-Chen model (right).

For both systems, Figure 8 displays the obtained results, showcasing Hopf, regular, conserved substrates, and chaotic behaviors. Depending on the control parameters (ϵ and c) of the two systems, their responses transition nonlinearly from steady state to periodicity, eventually leading to chaos. A homothetic transition exists in both the Lu-Chen and OEFB systems. The criticality of both systems may be very sensitive, quickly shifting between chaotic (unstable regime) and periodic (stable regime) states, making them challenging to control. However, once the feedback limit is exceeded, the system regains stability or coherency, facilitating easier regulation. A stable periodic limit cycle results from Hopf bifurcation in the Chen system due to the destabilization of a fixed point (Ming et al., 2010).

According to the results, nonlinear oscillators can be effectively controlled to create and manage chaos by incorporating most factors into the system, rather than solely adjusting frequency, as demonstrated in (Al Naimee, et al., 2021).

4. Conclusions

We conducted a study on the nonlinear transitions for chaotic system generation, comparing optoelectronic feedback (OEFB) and the Lu-Chen electronic chaotic systems under controlled parameters and initial conditions. In the OEFB scenario, the presence of mixed-mode oscillations (MMOs) during transitions and slow-fast chaotic regimes was observed. Both systems' behaviors were analyzed through FFT and attractors corresponding to time series, revealing a shared characteristic with a homoclinic orbit. Both systems exhibited excessive sensitivity to initial conditions and displayed dynamic nonlinear behavior, dependent on changes in certain controlling factors. This behavior was evident in the bifurcation patterns of both systems. The Lu-Chen system distinguishes itself from OEFB by featuring a multiscroll attractor, whereas OEFB displays a single scroll that meets the Shil'nikov condition, ensuring the existence of horseshoe chaos. This work contributes to the utilization of this potential chaotic system in secure communications.

The limitations of this work include:

1. **Limited Scope:** The study compares explicitly optoelectronic feedback (OEFB) and Lu-Chen electronic chaotic systems under controlled parameters and initial conditions. As such, the findings may not be generalizable to other chaotic systems or scenarios.
2. **Simplified Conditions:** The study may oversimplify real-world conditions using controlled and initial parameters. Real-world chaotic systems often exhibit complex interactions and variability that may not be fully captured in controlled experimental setups.
3. **Dependency on Controlling Factors:** The observed dynamic nonlinear behavior of both systems is stated to be dependent on changes in certain controlling factors. However, the specific factors and their impact on system behavior must be clearly defined and explored in-depth.
4. **Generalizability:** The findings may need to be revised in their applicability to broader contexts beyond the specific chaotic systems and conditions investigated in the study. Extrapolating the results to different systems or scenarios may require further research and validation.
5. **Complexity of Chaotic Systems:** Chaotic systems are inherently complex and can exhibit unpredictable behavior, sensitivity to initial conditions, and nonlinear dynamics. Understanding and characterizing these systems may require more comprehensive analyses and modeling approaches.

Future Research Directions: While the study provides valuable insights into the behavior of the studied chaotic systems, it suggests potential avenues for future research to explore additional factors, phenomena, or applications.

Acknowledgment

The research leading to these results has received no Research Grant Funding.


Author contribution: All authors have contributed, read, and agreed to the published version of the manuscript results.

Conflict of interest: The authors declare no conflict of interest.

References

- [1]. Algaba, A., Fernández-Sánchez, F., Merino, M., & Rodríguez-Luis, A. J. (2013). Chen's attractor exists if Lorenz repulsor exists: The Chen system is a special case of the Lorenz system. *Chaos: An Interdisciplinary Journal of Nonlinear Science*, 23(3), 033108.
- [2]. Al Naimee, K. A., & Yaseen, S. K. (2021). Experimental evidence of chaotic resonance in semiconductor laser. *Baghdad Science Journal*, 18(1 (Suppl.)), 0784-0784.
- [3]. Chengui, G. R. G., Jacques, K., Wofo, P., & Chembo, Y. K. (2020). Nonlinear dynamics in an optoelectronic feedback delay oscillator with piecewise linear transfer functions from the laser diode and photodiode. *Physical Review E*, 102(4), 042217.
- [4]. Chow, W. W., Koch, S. W., & Sargent, M. I. (2012). *Semiconductor-laser physics*. Springer Science & Business Media.
- [5]. Dina Ahmed Kaft, Raied Kamel Jamal, K. A. Al- Naimee. (2016) Lorenz model and chaos masking /addition technique. *Iraqi Journal of Physics*, Vol.14, No.31, PP. 51-60.
- [6]. Doungmo Goufo, E. F. (2018). Mathematical analysis of peculiar behavior by chaotic, fractional and strange multiwing attractors. *International Journal of Bifurcation and Chaos*, 28(10), 1850125.
- [7]. Hamadi, I. A., Jamal, R. K., & Mousa, S. K. (2022). Image encryption based on computer generated hologram and Rossler chaotic system. *Optical and Quantum Electronics*, 54(1), 33.
- [8]. Ibrahim, R. I., Al Naimee, K. A., & Yaseen, S. K. (2021). Ex- perimental Evidence of Chaotic Resonance in Semiconductor Laser. *Baghdad Science Journal*, 18(1).
- [9]. Jacquot, M., Lavrov, R., & Larger, L. (2010). Nonlinear delayed differential optical phase feedback for high performance chaos communications. In *CLEO/QELS: 2010 Laser Science to Photonic Applications* (pp. 1-2). IEEE.
- [10]. Jamal, R. K., & Abdulaali, R. S. (2022). A Comprehensive Study and Analysis of the Chaotic Chua Circuit. *Iraqi Journal of Science*, 556-570.
- [11]. Jamal, R. K., Ali, F. H., & Mutlak, F. A. (2021). Studying the chaotic dynamics using Rossler-Chua systems combined with a semiconductor laser. *Iraqi Journal of Science*, 2213-2221.
- [12]. Kadim, M. A., Tuaimah, A. N., Hassan, A. F., Abdalah, S. F., Meucci, R., Khidhir, A. H., & ALHusseini, H. (2023). Nonlinear quantum dot light emitting diode dynamics and synchronization with Optoelectronic feedback. *University of Thi-Qar Journal of Science*, 10(1).
- [13]. Li, X. F., Chlouverakis, K. E., & Xu, D. L. (2009). Nonlinear dynamics and circuit realization of a new chaotic flow: A variant of Lorenz, Chen and Lü. *Nonlinear Analysis: Real World Applications*, 10(4), 2357-2368.
- [14]. Li, X., Pan, W., Luo, B., & Ma, D. (2006). Control of nonlinear dynamics in external-cavity VCSELs with delayed negative optoelectronic feedback. *Chaos, Solitons & Fractals*, 30(4), 1004-1011.
- [15]. Liu, W., & Chen, G. (2003). A new chaotic system and its generation. *International Journal of Bifurcation and Chaos*, 13(01), 261-267.
- [16]. Luo, H., Cheng, M., Huang, C., Ye, B., Shao, W., Deng, L., ... & Liu, D. (2021). Experimental demonstration of a broadband optoelectronic chaos system based on highly nonlinear configuration of IQ modulator. *Optics Letters*, 46(18), 4654-4657.
- [17]. Lü, J., Chen, G., Cheng, D., & Celikovsky, S. (2002). Bridge the gap between the Lorenz system and the Chen system. *International Journal of Bifurcation and Chaos*, 12(12), 2917-2926.
- [18]. Ming, Z. X., Ju-Fang, C., & Jian-Hua, P. (2010). Theoretical and experimental study of Chen chaotic system with notch filter feedback control. *Chinese Physics B*, 19(9), 090507.
- [19]. Müller-Bender, D., Otto, A., Radons, G., Hart, J. D., & Roy, R. (2020). Laminar chaos in experiments and nonlinear delayed Langevin equations: A time series analysis toolbox for the detection of laminar chaos. *Physical Review E*, 101(3), 032213.
- [20]. Pehlivan, I., Ersin, K. U. R. T., Qiang, L. A. İ., Basaran, A., & KUTLU, M. (2019). A multiscroll chaotic attractor and its

- electronic circuit implementation. *Chaos Theory and Applications*, 1(1), 29-37.
- [21]. Raied Kamel Jamal, Dina Ahmed Kaft. (2016). Secure communications by chaotic carrier signal using Lorenz model. *Iraqi Journal of Physics*, Vol.14, No.30, PP. 51-63.
 - [22]. Ren, H. P., & Li, W. C. (2010). Heteroclinic orbits in Chen circuit with time delay. *Communications in Nonlinear Science and Numerical Simulation*, 15(10), 3058-3066
 - [23]. Saini, D. K. (2021). Fuzzy and mathematical effort estimation models for web applications. *Applied computing Journal*, 10-24.
 - [24]. Trikha, P., Jahanzaib, L. S., & Khan, A. (2022). Chaos control and fractional inverse matrix projective difference synchronization on parallel chaotic systems with application. In *Fractional-Order Design* (pp. 181-206). Academic Press
 - [25]. Ueta, T., & Chen, G. (2000). Bifurcation analysis of Chen's equation. *International Journal of Bifurcation and Chaos*, 10(08), 1917-19.
 - [26]. Wang, N., Li, C., Bao, H., Chen, M., & Bao, B. (2019). Generating multi-scroll Chua's attractors via simplified piecewise-linear Chua's diode. *IEEE Transactions on Circuits and Systems I: Regular Papers*, 66(12), 4767-4779.
 - [27]. Wei, Z., Pham, V. T., Kapitaniak, T., & Wang, Z. (2016). Bifurcation analysis and circuit realization for multiple-delayed Wang–Chen system with hidden chaotic attractors. *Nonlinear Dynamics*, 85, 1635-1650.

 Author(s) and ACAA permit unrestricted use, distribution, and reproduction in any medium, provided the original work with proper citation. This work is licensed under Creative Commons Attribution International License (CC BY 4.0).